

ELECTRICAL AND OPTICAL CHARACTERISTICS OF WATER UNDER HIGH ELECTRIC STRESS

S. Katsuki*[‡], R.P. Joshi, M. Laroussi, F. Leipold, and K.H. Schoenbach,

Physical Electronic Research Institute, Old Dominion University, Norfolk, VA 23529, USA

* Pulsed Power Laboratory, Kumamoto University, Kumamoto 860-8555, Japan

Abstract

In order to determine the electrical characteristics of water under high electric stress, we have measured the current-electric field (I - E) characteristics of distilled water with a resistivity of 200 k Ω cm, up to electric field intensities of 1 MV/cm. The gap between a 1.7 mm diameter sphere and a plane stainless steel electrodes was varied between 50 μ m to 400 μ m. Voltage pulses with duration of 200 ns and amplitude of up to 40 kV, provided by a 50 Ω Blumlein generator, were applied to the electrodes. In addition, measurements of changes in the index of refraction of distilled water under high electric stress were performed, using laser Schlieren method and Mach-Zehnder interferometry with a temporal resolution of one nanosecond.

With the electric fields in excess of 500 kV/cm the increase in the current was found to be super linear. This is in accordance with the general I - E characteristics for polar liquids. Optical measurements at average electric fields of up to 1 MV/cm revealed that a layer with decreased index of refraction emerges from the surface of the spherical electrode, which serves as anode. Shifting of the fringes is observed even after the voltage pulse ends. This might be an indication of change in composition of water after voltage applications.

I. INTRODUCTION

Water is widely used as an energy storage medium for pulsed power systems because of the high value of the relative dielectric constant of 81, and the high hold-off electric field which may reach values on the order of one MV/cm. Pulsed power systems using liquid storage media could be more compact and operate with a high repetition rate than conventional pulse power systems, and therefore be attractive for industrial applications. To minimize the system size, the electric field in the energy storage needs to be close to the critical value at which the electrical breakdown occurs. The electrical properties of liquids in such an intense pulsed electric field are still not well understood.

Theoretic studies on the electron kinetics in liquid argon under intense electric fields have shown that the electron drift velocity is nonlinearly dependent on the applied electric field [1]. A two-dimensional, percolative approach to model dielectric breakdown, based on a network of parallel resistor-capacitor elements having

random values, has recently been developed [2]. However, very few experiments on I - E characteristic of water were reported.

We have investigated the I - E characteristics of water using rectangular pulsed voltage with a duration of 200 ns. A quasi-homogeneous intense electric field up to 1 MV/cm is generated in a sphere to plane electrode sub-millimeter gap. Time resolved observations of the water under high electric stress are based on a Schlieren method and Mach-Zehnder interferometry.

II. EXPERIMENTAL SETUP AND PRODEDURE

Figure 1 shows a stainless steel hemisphere and plane electrodes with a gap distance, d . The radius of hemisphere electrode is 0.85 mm, and the gap distance, d , can be varied from zero to 1 mm with an accuracy of 5 μ m. The hemisphere electrode is connected to the ground through a current viewing resistor. A plane electrode is the high potential electrode. Both electrodes' surfaces were polished using a chemical micro compound. Both electrodes are set in a 4-inch's cubic chamber with two glass windows on the opposite sides. The two windows allow us to optically access the electrodes. Water resistivity was approximately 200 k Ω cm. In order to keep the condition of water between the electrodes, water around the electrodes is sucked out using a pipette, and fresh water is directly poured into the region after every shot.

Figure 2 shows an experimental setup, which includes the voltage pulse generator, discharge chamber, and an electrical and a optical diagnostics. A Blumlein generator was assembled to deliver the pulsed voltage

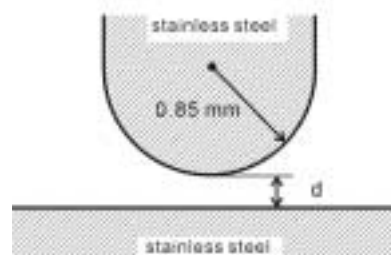


Figure 1. Hemisphere to plane electrode geometry. Negative or positive high voltage pulses are applied to the plane electrode; the hemispheric electrode is connected to ground. The gap distance d can be varied up to 1 mm with an accuracy of 5 μ m.

with duration of 200 ns to the electrodes in water. Since the generator consists of two 50 Ω coaxial cable (RG-217) in parallel, the output impedance of the generator is 50 Ω. The Blumlein generator is charged up to the voltage up to 30 kV using a DC high voltage power supply (Hipotronics). A 55 Ω resistor is placed at output terminal of the Blumlein for matching. Another 50 Ω resistor was inserted between the generator and the electrodes in order to increase the risetime of the voltage pulse. This allowed us to suppress the high frequency components of the pulse, which contribute to the electromagnetic noise in the detector systems.

The current flowing through the electrodes was measured by the shunt resistor (1.0 Ω), which consists of four low inductance resistors connected in parallel. The voltage across the gap is obtained using a high voltage probe (North Star Research Co.) with a frequency response of 250 MHz. An inductive voltage drop which is part of the signal is small enough to be neglected.

A Schlieren optical system using a 10 mW He-Ne laser and a fast gated ICCD camera (4Picos, Stanford Computer Researches) was built to observe the temporal behavior of water during voltage application. The expanded laser beam with a diameter of approximately 3 mm covers the space between the electrodes and the two windows. In order to synchronize the ICCD camera with the voltage pulse, the ICCD camera is triggered using a signal from pickup coil detecting the magnetic field from the triggered spark gap switch, TSG. Also a Mach-Zehnder interferometer was used to evaluate the change in index of refraction in water. In this experiment, temporal resolution of the optical system is 1 ns.

III. RESULTS AND DISCUSSION

A. Electrical properties of water between sphere-plane electrodes

Figure 3 shows the temporal development of voltage, current and displacement current, which was obtained by differentiating the voltage ($C_g dV_g/dt$). Comparing current and displacement current allowed us to obtain the value of the capacitance between the electrodes. It is 24 pF for the gap distance of 200 μm. As shown in Fig. 3, most of the measured current is displacement current. The fluctuation in the voltage waveform, which causes the oscillation in the displacement current, is caused by the stray capacitances in the discharge chamber. The resistive current, I_g , is defined as the current at a time when the voltage reaches a constant value, V_g . As shown in Fig. 3, this is approximately at $t = 180$ ns. Since $I_g = 0.13$ A, the resistance of the water between electrodes is 44 kΩ in this case. The values of resistance and the capacitance between the hemispherical and the plane electrode for various gap distances are shown in Fig. 4. for an electric field of 400 kV/cm. The dotted line shows the calculated resistance between plane electrodes with a cross section of $\pi \cdot 0.085^2$ cm². The fact that the measured resistance is not proportional to the gap distance is due to the electrode geometry in our experiments. For an hemispherical-plane

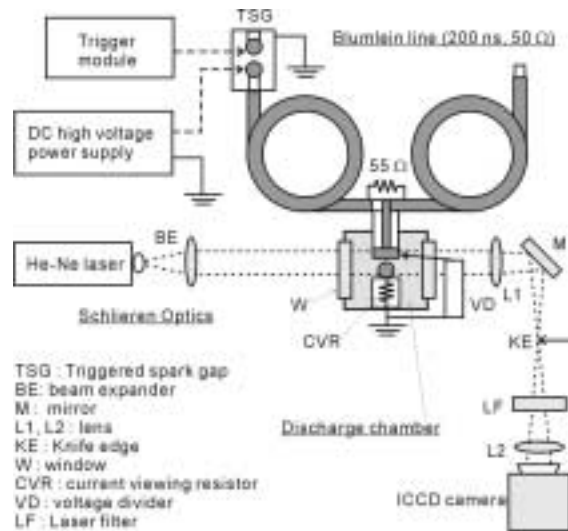


Figure 2. Experimental setup with Schlieren system.

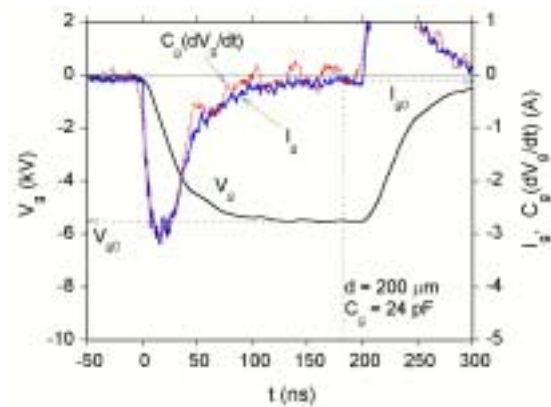


Figure 3. Example of waveforms of the voltage, V_g , current, I_g , and displacement current, obtained by differentiating the voltage ($C_g(dV_g/dt)$), for the gap distance of 200 μm.

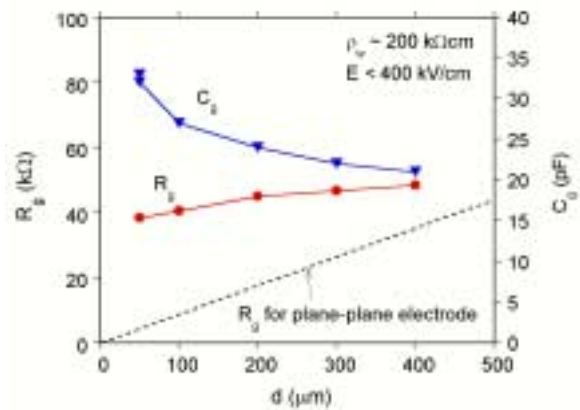


Figure 4. Resistance and capacitance between electrodes as a function of gap distance, d .

electrode geometry the radial current distribution between the electrodes changes for different gap

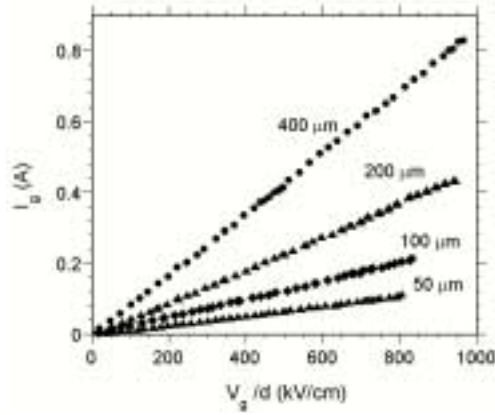


Figure 5. Relation between the resistive current and the maximum electric field (I - E characteristics) for the various gap distances.

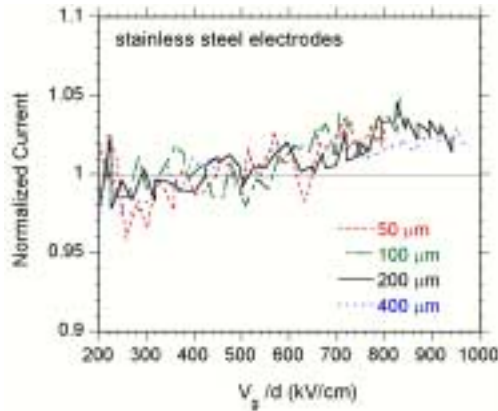


Figure 6. Resistive current between electrodes, normalized by $(V_g/d)/R_g$, as a function of applied electric field.

distances. For the short gap distances, where the current concentrates in the center region, the effective cross section for the current is smaller than for larger distances. Therefore, the resistance per unit length along the gap becomes larger.

Figure 5 shows the relation between the resistive current and the maximum electric field, E_m , which is defined as V_g/d (I - E characteristic), for the gap distances of 50, 100, 200 and 400 μm . The relations between the current and electric field for all gap distances appear to be linear. However, by plotting the current normalized with respect to $(V_g/d)/R_g$, (Figure 6) where R_g is the value in Fig. 5, an increase in normalized current above the value, which is based on the assumption of a constant resistance, is seen for $E > 500$ kV/cm.

B. Temporally resolved Schlieren photography and interferometry

Figure 7 shows the Schlieren and interference images of water between the electrodes with the gap distance of 400 μm before and 200 ns after the beginning of the voltage pulse. At 200 ns after the voltage application, a dark region surrounding the sphere electrode is observed.

From other experiments, it is known that the interference fringes shifting downward indicate a decrease in the index of refraction. When the polarity of the hemispherical electrode is changed to negative, this pattern stays the same. Therefore, the polarization does not seem to play an important role on the observed change in refractive index. It is more likely the value of the electric field, which is higher near the hemispherical electrode than near the plane electrode, which causes this effect (Kerr effect).

Figure 8 shows the temporal development of the change in the index of refraction in the water gap. Although each image was taken from a different discharge, the sequence of images is fairly reproducible. At $t = 70$ ns a dark region emerges from the high field electrode. This region expands and propagates toward the plane electrode. Figure 9 shows the distribution of the relative index of refraction along the electrode axis, which is obtained from the Schlieren images in Fig. 8. The index of refraction is integrated along the laser beam direction (normal to the electrode axis). After the voltage application the refractive index near the hemispherical electrode decreases with increasing distance to the electrode. The region with decreased refractive index, which is called “striation” in this paper, gradually expands to the plane electrode. The distribution with the decreased refractive index near the hemisphere electrode is similar to the interferometer fringe pattern near the electrode axis at 200 ns in Fig. 7. The striation is still moving even after the voltage pulse ends. At $t = 220$ ns, the refractive index near the sphere electrode begins to increase. After a while the gradient of the refractive index is inverted. The axial velocity of the striation is approximately 1.6 km/s similar to the sound velocity in water. This seems to indicate that the observed change in the index of refraction at the hemispherical electrode, which is obviously caused by the high electric field at this electrode, generates a localized mechanical stress (Maxwell stress), which causes the launching of an

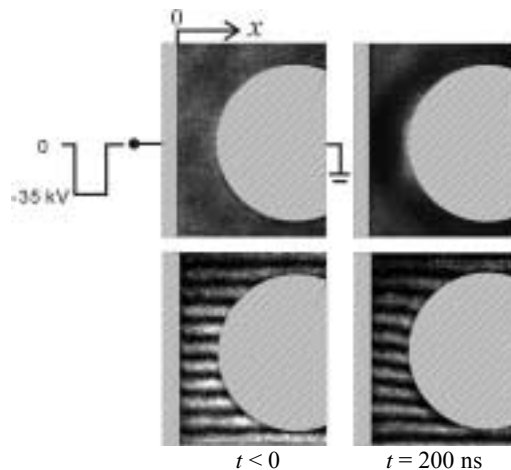


Figure 7. Schlieren (above) and interference (lower) images between the electrodes before and 200 ns after the beginning of voltage application. $d = 400$ μm .

acoustic wave. This striation is observed only for electric fields in excess of 500 kV/cm, which is the same range where the I - E characteristic becomes super-linear.

IV. SUMMARY

Electric fields of up to 1 MV/cm are applied to water between a hemispherical and plane electrode with a sub-millimeter gap distance. The I - E characteristic of the water is linear for electric fields of less than 500 kV/cm, and increases super-linearly with electric field exceeding 500 kV/cm. In this electric field range (> 500 kV/cm) striations, regions with decreased refractive index, emerge from the hemispherical electrode and propagate in form of acoustic waves towards the plane electrode. Electric fields of this magnitude seem to influence the electrical property of water.

ACKNOWLEDGEMENTS

This research has been supported by an AFOSR/DOD MURI grant on Compact, Portable Pulsed Power, administered through the University of New Mexico.

REFERENCES

- [1] E.E. Kunhardt, "Electron kinetics in simple liquids at high electric fields," *Phys. Rev. B*, vol. 44, no. 9, pp. 4235-4244, 1991.
- [2] R.P. Joshi, J. Qian, S. Katsuki, K.H. Schoenbach, and E. Schamiloglu, "Electrical Conduction in Water Revisited: Roles of Field Enhanced Dissociation and a Reaction-Based Boundary Condition," to appear in *IEEE Trans. Dielectr. Electr. Insulat.*
- [3] S. Katsuki, S. Xiao, R. P. Joshi, M. Laroussi, and K. H. Schoenbach, "Electrical breakdown of sub-millimeter water gaps," to appear in the *Proc. Of the International Power Modulator Symposium, 2002, Los Angeles, USA.*

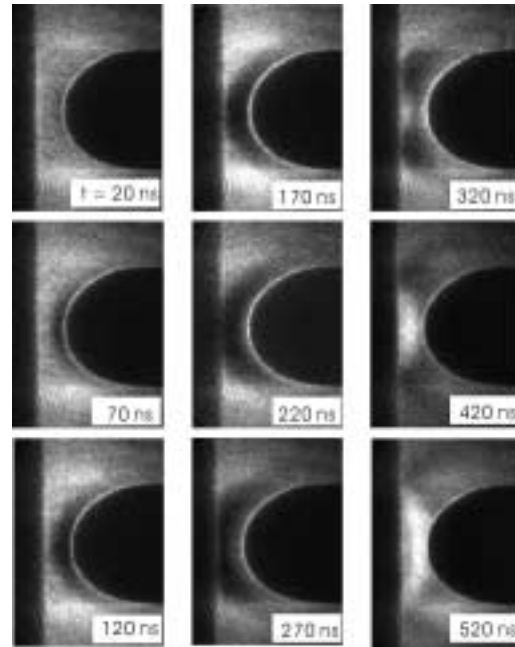


Figure 8. Temporally resolved Schlieren images of a water gap with gap distance of 40 μm and average electric fields of 900 kV/cm. The number in each image shows the time from the beginning of the voltage pulse.

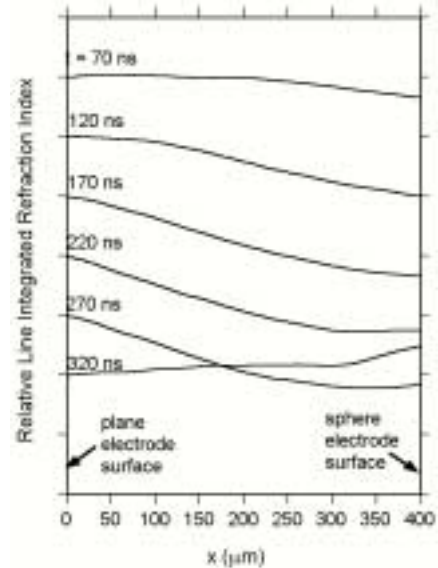


Figure 9. Temporal development of spatial distribution of refraction index of water between electrodes.